Erosion of biofilm-bound fluvial sediments

Elisa Vignaga[1], David M. Sloan[2], Xiaoyu Luo[3], Heather Haynes[4], Vernon R. Phoenix[5] and William T. Sloan[1]*

The movement of fluvial sediment shapes our rivers. Understanding sediment entrainment has been a goal of hydraulic engineers for almost a century[1,2]. Previous sediment entrainment models have been informed by laboratory experiments using grains that were free from biological material[3]. In natural river settings, however, sediments are invariably covered by bacteria, often forming visible biofilms, which comprise diverse consortia of species housed in sticky extracellular polysaccharides. Here we report experiments in a laboratory flume with cyanobacteria grown over sediment. We show that the prevailing model, where grains roll over one another at some critical threshold in shear velocity, does not hold for biofilm-bound sediments. Instead, biostabilized sediment behaves more like an elastic membrane. Fluid flow produces oscillations in the membrane, which can become unstable. Beyond a particular threshold in velocity, the membrane fails catastrophically by ripping and clumps of biofilm-bound sediment become entrained. We use a mathematical model of an oscillating membrane in incompressible flow to show that unstable oscillations will occur over a wide range of elastic material properties at realistic river flow velocities. We find that the horizontal length scale over which oscillations occur is a controlling factor for incipient sediment entrainment of biostabilized sediments.

Sediments have a huge impact on natural fluvial processes and on human exploitation of rivers. Scour, transport and deposition of sediment can act to render expensive infrastructure, such as bridges and dams, useless and transport pollutants large distances from their source. However, sediments also harbour rich biological communities that recycle nutrients and remove contaminants. Therefore, the ability to predict the transport of fluvial sediments has far-reaching applications from conservation to river basin management and civil engineering design. Thus conceptual and ultimately mathematical models of the energy dissipation and entrainment mechanisms when river flows and sediment interact are critical in predicting sediment movement.

It has been shown that it can take up to five times higher shear stress to entrain biofilm-bound marine sediments than clean ones[4]; the phenomenon had been called biostablization[5,6]. It seems to be widespread and potentially reflects a stratagem that has evolved independently in different clades of bacteria to convey an advantage on early colonizers[7]. The ubiquity of biostabilization has had little impact on practical prediction of sediment transport where empirical models, parameterized using clean sediments in laboratories, prevail despite being found wanting in real-world rivers[8].

We inoculated an incubation flume with cyanobacteria *Phormidium* sp. where the bacteria colonized trays of sand with 1.2 mm median diameter, 1 mm glass beads or 2.2 mm gravel on the bed of the flume. Filamentous cyanobacteria are a common component of fluvial sediment communities[9,10]. The bacteria grew rapidly, excreted extracellular polysaccharides and adhered to the sediment grains to form a composite mat-like material. At various stages of growth over a ten-week period trays were removed and placed in a test flume. In one set of experiments a glass lid was lowered onto the free surface for filming the motion of the bed with a high-resolution camera; in a second the free surface was maintained and high-resolution particle imaging velocity metering was used to characterize the hydraulics. The flow was ramped up in discrete steps and the biofilm was imaged at each plateau. However, it rapidly became apparent that long-established methods based on the frequency of movement of individual grains[11] are poor predictors of entrainment in biostabilized sediments. The biofilm–sediment composite membrane began to oscillate in the flow until it eventually ripped and a chunk of biofilm and grains was washed away (Supplementary Movies S1 and S2). The maximum increase in the time-averaged shear stress required to entrain these biofilm-covered sediments over and above that for clean sediments[11] was 43% for the glass beads, 35% for gravel and 30% for sand[12]. Thus, cyanobacteria can have a significant stabilizing effect on these non-cohesive sediments, which are typical of rivers. The composite biofilm–sand and biofilm–bead materials were sufficiently strong that we could remove strips of them from the flume and load test (Supplementary Movie S3) them in a 5 N load cell where they exhibited elastic behaviour. We calibrated finite element models of the tests which gave a Young's modulus of elasticity of approximately 10 kPa for bead composites and 7.2 kPa for sand (Supplementary Fig. S1). Although the biofilm–gravel material seemed to be strong, the weight of the gravel grains meant that the composite material could not be removed intact from the flume for load testing.

Compared with previously measured biofilm material properties from other environments[13] our *Phormidium* sp. biofilm seems to be at the strongest end of a very wide range. Most real-world fluvial biofilms will comprise a diverse consortium of species and thus potentially possess a wide range of material properties. Therefore, we use a mathematical model to test whether our conceptual model of a fluttering membrane becoming unstable and ultimately ripping above a threshold in flow velocity is theoretically feasible, and potentially generic.

Figure 1 gives schematic diagrams of an elastic composite comprising sediment and biofilm. We assume that the flow is described by the Navier–Stokes equations and carry out a linear stability analysis focusing on the effects that perturbations, u, about a mean laminar profile, U, have on the motion of the elastic membrane. Flows considered here will be turbulent and one might be tempted to base an analysis on perturbations about a different time-average flow profile. This would require a suite of assumptions

---

[1]School of Engineering, University of Glasgow, G12 8QQ, UK, [2]Department of Mathematics, University of Strathclyde, G1 1XQ, UK, [3]School of Mathematics and Statistics, University of Glasgow, G12 8QQ, UK, [4]School of the Built Environment, Heriot Watt University, EH14 1AS, UK, [5]School of Geography and Earth Sciences, University of Glasgow, G12 8QQ, UK. *e-mail: william.sloan@glasgow.ac.uk

on indeterminate and velocity-dependent length scales. However, another study[14] considered various basic flow profiles consistent with high Reynolds number flow in a flexible channel: it concluded that varying the profile made no qualitative difference to the stability characteristics. Furthermore, it has been common practice since the early classical work in fluid mechanics[15,16] for laminar profiles to be used to give guidance on the onset of instabilities even when turbulence is present. The perturbations are composed of wave-like modes with spatial wave number α; if the membrane is anchored at either end of a length L then wave numbers can be only $2\pi n/L$, where n is an integer. The problem of seeking unstable modes becomes one of looking for the eigenvalues of the Orr–Sommerfeld equation, with boundary conditions defined by the moving elastic membrane and the upper free or no-slip surface, that 'blow up' with increasing time. Ref. 17 first explored the rich behaviour of the eigenmodes of the Orr–Sommerfeld equation with compliant boundaries and the model we use, which is based on this and that presented by ref. 18, is explained and solved numerically in the Supplementary Information using methods adapted from ref. 19. Two different scenarios are considered. In both, the lower boundary is our elastic composite membrane that is loosely anchored to the underlying substratum; in one the upper boundary allows no fluid motion, which is akin to our laboratory experiment where we have glass plate at the water surface (Fig. 1a). In the other the upper boundary is a free surface with no applied shear stress and atmospheric pressure (Fig. 1b). We consider the two different composite membranes for which we measured the material properties (Table 1). These material properties are not routinely measured for biotic sediments but as they become available the analysis can easily be extended to biofilms with different consortia of species.

Figs 2 and 3 give the neutral stability curves for the eigenmodes (oscillations) of our model as a function of α and the Reynolds number, $R = U_0 h/\nu$, where U_0 is the centreline velocity, h is half the channel depth and ν kinematic viscosity coefficient. For parameter values to the right of the curves, oscillations are unstable and 'blow-up' with time and to the left they diminish. When the channels have solid boundaries then only one unstable mode exists; the much studied Tollmien–Schlichting instability that heralds the onset of turbulence in the transition from laminar flow. When we make the bottom boundary compliant then a second mode of instability appears, which has been called travelling wave-flutter (TWF) instability[18].

Consider first the capped flume used to image the oscillating membrane and erosion. For both composites one of the effects is to reduce the area of the parameter space associated with Tollmien–Schlichting instability (Fig. 2). Thus, there is a degree of flow stabilization in the flow afforded by the compliant wall. However, TWF instability exists for a large range of wave and Reynolds numbers; we know this instability is associated with the compliant wall because introducing damping to our wall equation stabilizes this mode but has no effect on the Tollmien–Schlichting instability. A previous study[20] showed by explicitly modelling the interaction of flow and a similar elastic membrane that the energy transferred to and dissipated by an oscillating membrane can be substantial. It has been demonstrated[21] that oscillations in biofilm streamers can occur even in low Reynolds number flows. Unsurprisingly, for the stiffer glass-bead composite the region associated with TWF is smaller than for the weaker sand composite. We were able to measure the wavelength of oscillation before membrane failure in four experiments with differing flow conditions; three for glass-bead composites and one for sand composite (Table 1). When we plot the wave number verses Reynolds number at the point of membrane failure all four lie within the unstable region for TWF. Despite the sand–biofilm composite being the least stiff membrane in our experiment it failed at the highest Reynolds number because
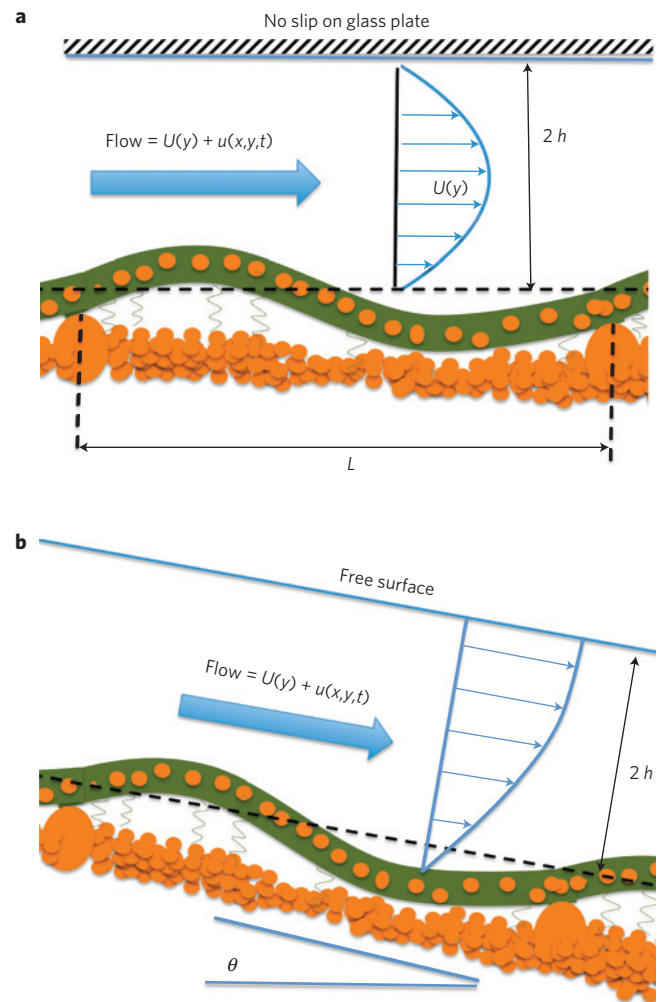

Figure 1 | Schematic diagrams of fluid flow in our flumes causing an elastic composite of sediment grains and biofilm on the bed to oscillate. The composite is loosely bound to the substratum by filaments of biofilm. We decompose the flow into a mean profile, $U(y)$, with perturbations, $u(x,y,t)$, superimposed. x and y are distance downstream and perpendicular to the mean flow, respectively, and t is time. The eigenvalues of the Orr–Sommerfeld equation (Supplementary Information) are then used to determine when the perturbations become unstable, grow and cause the membrane to rip. **a**, Our model for the capped flume has a no-slip upper boundary. **b**, For the open channel, we have a free surface boundary with no applied shear (Supplementary Information).

the wavelength of oscillation was approximately half that observed for bead composites.

When we have open channel flow the Tollmien–Schlichting instability completely disappears and only TWF instabilities remain over a smaller region than for the capped flume (Fig. 3). Thus the open channel with compliant lower boundary seems to be a slightly more stable system. We were unable to image the oscillating membrane through the free surface to determine the wavelength immediately before membrane failure. However, when we use particle image velocity metering to map the velocity fields above beds of glass beads or gravel that are free from biological material and compare them with the fields above these beds when an extensive biofilm has been allowed to develop, then the stabilizing effect of the biofilms is readily apparent (Fig. 4). The standard deviation in the vertical component of flow is significantly lower when a biofilm is present, indicating a reduction in vertical oscillations. For the gravel bed the acceleration in the flow across the field of view is less when the

Table 1 | The material properties and the conditions at point of failure of two different elastic composite membranes comprising glass beads or sand and *Phormidium* sp. biofilm that formed on the bed of the flumes.

Composite material	Material properties			Conditions at point of failure				
	Young's modulus (Pa)	Thickness (m)	Poisson's ratio	Test	R	2h (m)	L (m)	α
Glass-beads–biofilm	10,000	0.0022	0.4	1	6,562	0.035	0.076	2.9
				2	4,867	0.0295	0.032	2.9
				3	8,505	0.042	0.028	4.7
Sand–biofilm	7,200	0.002	0.4	4	9,881	0.043	0.025	5.3

R is the Reynolds number, 2h is the flow depth and L and α are the wavelength and wave number of membrane oscillation respectively.
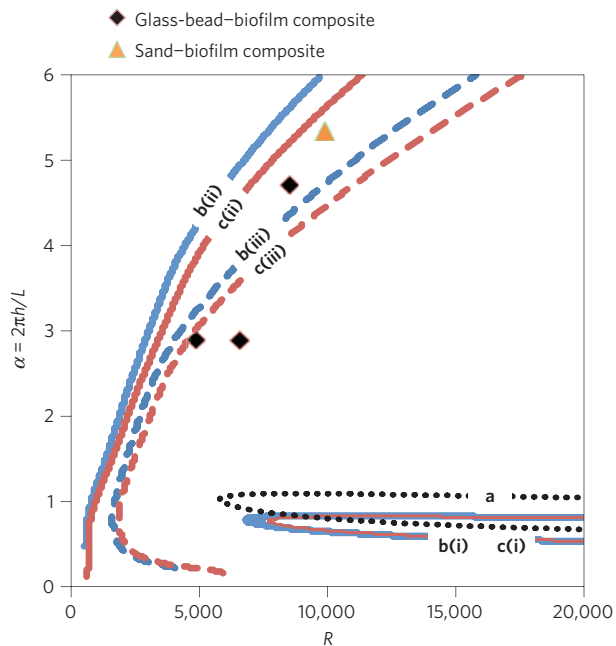

Figure 2 | Neutral stability curves predicted for perturbations in the capped flume (Fig. 1a) with biofilm–sand (blue) and biofilm–bead (red) composite properties given in Table 1. Two different types of instability prevail: classical Tollmien–Schlichting (TS) instability in the bulk flow and travelling wave-flutter (TWF), which is associated with a compliant elastic wall. **a**, TS for a solid bed; **b(i)**, TS for sand composite; **b(ii)**, TWF for sand composite; **b(iii)**, TWF for sand composite with damping coefficient $d = 10$; **c(i)**, TS for glass-bead composite; **c(ii)**, TWF for glass-bead composite; and **c(iii)**, TWF for glass-bead composite with damping. The markers indicate the α and R values at which the membranes were observed to fail in the experimental flume; all lie in the predicted unstable flow regions to the right of the neutral stability curves.

biofilm is present, indicating that, despite lower turbulence, more energy is being extracted from the flow than for the biofilm-free bed, which on visual inspection seems to be rougher. Energy expended moving the membrane may account for this. For the glass-bead bed, the reduced vertical fluctuation in flow associated with the presence of the biofilm is not accompanied by reduction in flow speed. Therefore, the relative importance of the mechanical movement of the membrane and friction and turbulence on the energy extracted from the flow differs between the different composites. These effects of biofilm coverage might be encapsulated by calibrating situation-specific roughness lengths, but roughness length is a fickle parameter, born out of a desire to interpret macroscopic flow behaviour, which varies with a multitude of microscopic processes that defy characterization. The movement of grains in an elastic membrane may be one such process that can ultimately be quantified.
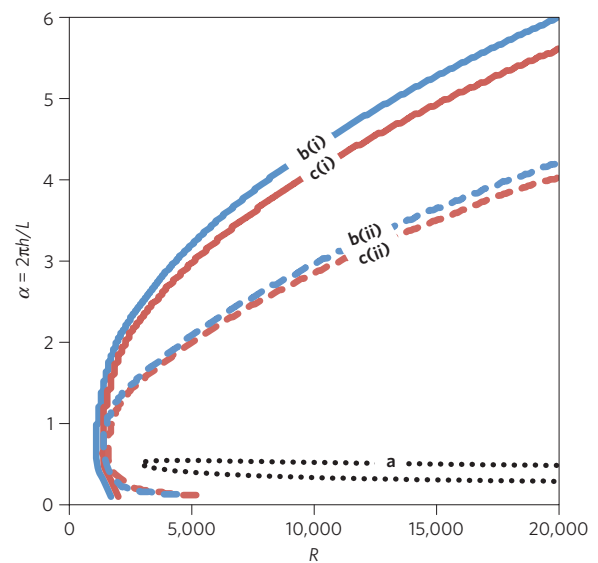

Figure 3 | Neutral stability curves predicted for perturbations in the open flume (Fig. 1b) with sand–biofilm (blue) and bead–biofilm (red) composite properties given in Table 1. a, TS instabilities are apparent only when there is a fixed bed, they disappear in the open channel when there is a compliant bottom boundary. **b(i)**, TWF for sand composite; **b(ii)**, TWF for sand composite with damping; **c(i)**, TWF for glass-bead composite; and **c(ii)**, TWF for glass-bead composite with damping.

Our observation that biofilm-bound fluvial sediments break off in clumps echoes that of a previous study[4] on marine sediments. Thus biofilms cause non-cohesive sediments to become cohesive, thereby changing the mechanism of bed failure from local, which can be evaluated from forces and torques on individual grains, to non-local, involving many linked grains. Despite the growing understanding of the factors affecting cohesive sediments, a mechanistic model that can predict the erodibility of cohesive sediment has proved elusive[23]. By observing the incipient pre-entrainment behaviour of the biofilm–sediment composite and through mathematical modelling we have suggested a model of sediment entrainment whereby instabilities in the flow and membrane grow until the membrane fails catastrophically. The effects of bacterial biofilms on fluvial sediment transport have hitherto been ignored in predictive models but biofilms are ubiquitous and will inevitably form elastic bonds between grains on a riverbed. Therefore, synchronized mechanical oscillation will always influence the hydrodynamics and the mechanisms of sediment entrainment. Our results suggest that relative influence of this in comparison with more widely acknowledged modes of entrainment could ultimately be predicted if material properties of the biofilm-bound sediments are known. Furthermore, we also demonstrated that the wavelength of a biofilm oscillation is critical.
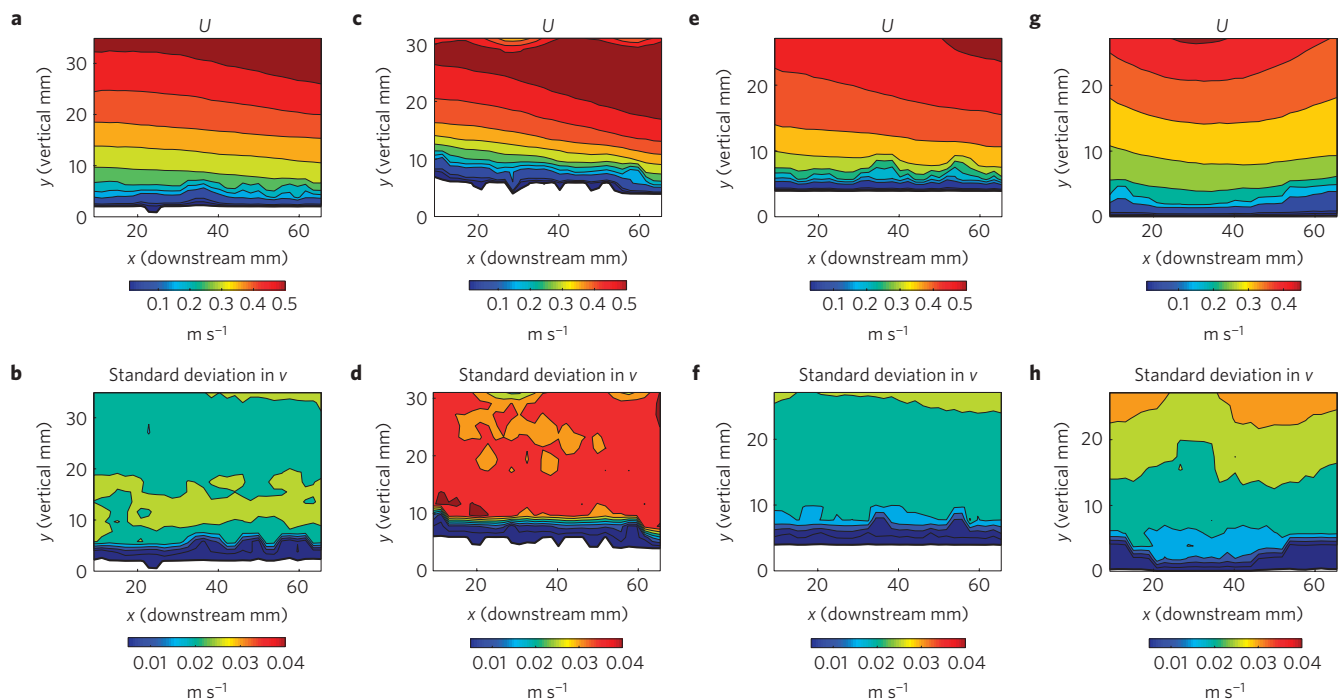
Figure 4 | The flow velocity in a section down the centre line of the open channel flume was recorded using PIV. The top row gives the horizontal component of velocity averaged over five seconds and the bottom row gives the standard deviation of the vertical component of velocity for the same period. **a,b,** Over a gravel–biofilm composite with $R \sim 8,200$; **c,d,** For the same flow rate over only gravel. **e,f,** Over a glass-bead–biofilm composite with $R \sim 5,940$; **g,h,** For the same flow rate over only glass beads. The presence of a biofilm has a significant calming effect on vertical perturbations in the flow.

So, for example, small patches that are typical of early colonization can sustain only short-wavelength oscillations and are therefore more stable than large patches of mature biofilm, where long-wavelength oscillations can occur. The conventional wisdom is that vertical roughness scales determine the propensity for non-cohesive sediments to become entrained; our findings suggest that a measure of the horizontal extent of biofilm coverage may be an important indicative scale for predicting the entrainment of sediment bound by strong biofilms.

Methods

Modelling. The description of the modelling has been placed in the Supplementary Information but this should not belie its importance. Our model of instabilities in membrane-like, bacterially bound fluvial sediments is new and we developed a bespoke numerical solution scheme to solve the partial differential equation that describes it.

Development of biofilm. In separate experiments we placed 0.02-m-deep trays of glass beads, sand and gravel on the base of our incubation flume (4 m long × 0.6 m wide), which we inoculated with cyanobacteria *Phormidium* sp. Water, supplemented with growth medium[22], was circulated at a rate calculated to generate a shear stress that was 50% of the critical shear stress according to the sediment size[11]. The growth took place for up to ten weeks under a light cycle of 12 h photosynthetically active radiation of 26 μmol m^{-2} s^{-1} followed by 12 h darkness. Temperature was held constant at 28 °C.

Imaging flow. Two test flumes were used: a 15 m long × 0.3 m wide, capped flume and a 5 m long × 0.3 m wide for open channel flow and particle image velocimetering (PIV) analysis, both with a slope of 1/200 with the tailgate adjusted to make the flow as uniform as possible over an immobile bed. Trays were removed at various stages of growth, without replacement, from the incubation flume and placed in the testing flumes. In the capped flume the flow was ramped up in discrete steps such that the applied fluid shear stress ranged from 0.69 Pa ($R = 3,200$) to a maximum of 2.24 Pa ($R = 24,800$); at each step the flow was held constant for 5 min for sand and 10 min for beads and gravel. The motion of the biofilm and subsequent erosion patterns were observed using a high-resolution digital camera (Sony HDR-SR5E 4 megapixel). In the open-channel flow experiments the shear stress ranged from 0.88 Pa ($R = 4,000$) to a maximum of 2.90 Pa ($R = 27,400$). We used a DANTEC PIV system (Supplementary Table S1) to map the flow velocity in a horizontal plane parallel to the streamlines in the centre of the flume. The

frequency of image capture was adjusted for flow rate (Supplementary Table S2) but on average 2,000 images were captured during approximately five seconds over an area of 60 mm × 30 mm resolved into 1,000 × 500 pixels.

Load testing. Load testing was conducted on a 5 N Tinius Olsen H1KS tensile tester. Strips of composite material were transported to the load cell in water to prevent them from drying out. A constant displacement rate of 1.6 μm s^{-1} was applied.

References

1. Gilbert, G. K. *The Transportation of Debris by Running Water* (United States Geological Survey, 1914).
2. Shields, A. *Application of Similarity Principles and Turbulence Research to Bed-load Movement* (US Dept. of Agr., Soil Conservation Service Cooperative Laboratory, California Institute of Technology, 1936).
3. Gomez, B. & Church, M. An assessment of bed load sediment transport formulae for gravel bed rivers. *Wat. Resour. Res.* **25,** 1161–1186 (1989).
4. Grant, J. & Gust, G. Prediction of coastal sediment stability from photopigment content of mats of purple sulfur bacteria. *Nature* **330,** 244–246 (1987).
5. Black, K. S., Tolhurst, T. J., Paterson, D. M. & Hagerthey, S. E. Working with natural cohesive sediments. *J. Hydraul. Eng.-Asce* **128,** 2–8 (2002).
6. Paterson, D. M. in *Cohesive Sediments* (eds Burt, N., Parker, R. & Watts, J.) 215–229 (1997).
7. Garcia-Pichel, F. & Wojciechowski, M. F. The evolution of a capacity to build supra-cellular ropes enabled filamentous cyanobacteria to colonize highly erodible substrates. *PLoS ONE* **4.11,** e7801 (2009).
8. Bathurst, J. C. Effect of coarse surface layer on bed-load transport. *J. Hydraul. Eng.-Asce* **133,** 1192–1205 (2007).
9. Wilhelm, L., Singer, G. A., Fasching, C., Battin, T. J. & Besemer, K. Microbial biodiversity in glacier-fed streams. *Isme J.* (2013) Early on line.
10. Lyautey, E., Lacoste, B., Ten-Hage, L., Rols, J. L. & Garabetian, F. Analysis of bacterial diversity in river biofilms using 16S rDNA PCR-DGGE: Methodological settings and fingerprints interpretation. *Water Res.* **39,** 380–388 (2005).
11. Yalin, M. S. & Karahan, E. Inception of sediment transport. *J. Hydraul. Div.-Asce* **105,** 1433–1443 (1979).
12. Vignaga, E. *The Effect of Biofilm Colonization on the Stability of Non-cohesive Sediments.* PhD thesis, Univ. Glasgow (2012).

13. Aggarwal, S., Poppele, E. H. & Hozalski, R. M. Development and testing of a novel microcantilever technique for measuring the cohesive strength of intact biofilms. *Biotechnol. Bioeng.* **105,** 924–934 (2010).
14. Xu, F., Billingham, J. & Jensen, O. E. Divergence-driven oscillations in a flexible-channel flow with fixed upstream flux. *J. Fluid Mech.* **723,** 706–733 (2013).
15. Benjamin, T. B. Shearing flow over a wavy boundary. *J. Fluid Mech.* **6,** 161–205 (1959).
16. Miles, J. W. On the generation of surface waves by shear flows. *J. Fluid Mech.* **3,** 185–204 (1957).
17. Benjamin, T. B. Effects of a flexible boundary on hydrodynamic stability. *J. Fluid Mech.* **9,** 513–532 (1960).
18. Davies, C. & Carpenter, P. W. Instabilities in a plane channel flow between compliant walls. *J. Fluid Mech.* **352,** 205–243 (1997).
19. Huang, W. Z. & Sloan, D. M. The pseudospectral method for solving differential eigenvalue problems. *J. Comp. Phys.* **111,** 399–409 (1994).
20. Liu, H. F., Luo, X. Y. & Cai, Z. X. Stability and energy budget of pressure-driven collapsible channel flows. *J. Fluid Mech.* **705,** 348–370 (2012).
21. Taherzadeh, D. *et al.* Computational study of the drag and oscillatory movement of biofilm streamers in fast flows. *Biotechnol. Bioeng.* **105,** 600–610 (2010).
22. Rippka, R., Deruelles, J., Waterbury, J. B., Herdman, M. & Stanier, R. Y. Generic assignments, strain histories and properties of pure cultures of cyanobacteria. *J. Gen. Microbiol.* **111,** 1–61 (1979).
23. Grabowski, R. C., Droppo, I. G. & Wharton, G. Erodibility of cohesive sediment: The importance of sediment properties. *Earth-Sci. Rev.* **105,** 101–120 (2012).

Author contributions

E.V. conducted the experimental research; E.V., H.H., V.R.P. and W.T.S. planned the experiments; X.L., D.M.S. and W.T.S. formulated the mathematics; D.M.S. was responsible for the numerics; W.T.S. undertook the computing and W.T.S. and D.M.S. wrote the paper.

Additional information

Supplementary information is available in the online version of the paper. Reprints and permissions information is available online at www.nature.com/reprints. Correspondence and requests for materials should be addressed to W.T.S.

Competing financial interests

The authors declare no competing financial interests.